Published in final edited form as:
Cell Mol Bioeng. 2010 June 1; 3(2): 151–162. doi:10.1007/s12195-010-0119-x.

Modification of Cellular Cholesterol Content Affects Traction Force, Adhesion and Cell Spreading

Leann L. Norman[1], **Ratna J. Oetama**[1], **Micah Dembo**[2], **F. Byfield**[3], **Daniel A. Hammer**[3,4], **Irena Levitan**[5], and **Helim Aranda-Espinoza**[1]

[1]Fischell Department of Bioengineering, University of Maryland, College Park, MD 20742, USA

[2]Department of Biomedical Engineering, Boston University, Boston, MA 02215, USA

[3]Department of Bioengineering, University of Pennsylvania, Philadelphia, PA 19104, USA

[4]Institute for Medicine and Engineering, University of Pennsylvania, Philadelphia, PA 19104, USA

[5]Pulmonary, Critical Care and Sleep Medicine, University of Illinois at Chicago, Chicago, IL 60612, USA

Abstract

Cellular cholesterol is a critical component of the plasma membrane, and plays a key role in determining the physical properties of the lipid bilayer, such as elasticity, viscosity, and permeability. Surprisingly, it has been shown that cholesterol depletion increases cell stiffness, not due to plasma membrane stiffening, but rather, due to the interaction between the actin cytoskeleton and the plasma membrane. This indicates that traction stresses of the acto-myosin complex likely increase during cholesterol depletion. Here we use force traction microscopy to quantify the forces individual cells are exerting on the substrate, and total internal reflection fluorescence microscopy as well as interference reflection microscopy to observe cell–substrate adhesion and spreading. We show that single cells depleted of cholesterol produce larger traction forces and have large focal adhesions compared to untreated or cholesterol-enriched cells. Cholesterol depletion also causes a decrease in adhesion area for both single cells and monolayers. Spreading experiments illustrate a decrease in spreading area for cholesterol-depleted cells, and no effect on cholesterol-enriched cells. These results demonstrate that cholesterol plays an important role in controlling and regulating the cell–substrate interactions through the actin–plasma membrane complex, cell–cell adhesion, and spreading.

Keywords

Plasma membrane; Lipid membrane; Endothelial cells; Cytoskeleton; Focal adhesions

INTRODUCTION

Cholesterol is one of the major lipid components of the plasma membrane, well known to be associated with multiple disorders, including atherosclerosis, lysosomal storage diseases (including Sandhoff, Tay-Sachs, and Niemann-Pick) and possibly Alzheimer's disease.[28] Numerous studies have shown that cholesterol regulates a variety of membrane proteins,

Address correspondence to Helim Aranda-Espinoza, Fischell, Department of Bioengineering, University of Maryland, Room 3138, Jeong H. Kim Engineering Building (Bldg. #225), College Park, MD 20742, USA. helim@umd.edu.
Associate Editor Yu-Li Wang oversaw the review of this article.

including multiple receptors and ion channels. [21,25,27,36,37] More recently, however, it became increasingly clear that cholesterol effects are not limited to changes in membrane structure and altering the function of membrane proteins, but that cholesterol also has major indirect effects on the cytoskeleton. Several lines of evidence indicate that changes in membrane cholesterol can indirectly alter biochemical properties of the cytoskeleton and its association with the plasma membrane: (a) multiple studies have shown that cholesterol-rich membrane domains (lipid rafts) serve as focal points for membrane–cytoskeleton interactions[26]; (b) depletion of membrane cholesterol increases cellular stiffness of endothelial cells,[5] an effect that is the opposite to the expected changes in membrane lipid bilayer where cholesterol depletion results in a reduction in bilayer thickness[8] and a decrease in membrane stiffness in artificial lipid layers [30]; (c) cholesterol depletion also increases contractile forces generated by the cells in 3D collagen matrix[6] and (d) strengthens membrane–cytoskeleton adhesion. [46] Cholesterol depletion also facilitates shear stress-induced realignment of endothelial cells, as well as individual F-actin fibers, in the direction of flow.[23] Interestingly, reported effects of cholesterol depletion on stress fibers have varied, with one group showing a decrease in the size of stress fibers in human fibroblasts[24]; while alternatively, no differences in actin intensity were reported for cholesterol depleted bovine aortic endothelial cells.[5] Differences in cell type, depletion times, and vehicle treatment for control cells are all factors which may contribute to these differences.

One possibility to explain the above mentioned increase in cell stiffness is that it is due to a decrease in actin turnover leading to the stabilization of the membrane–cytoskeleton complex.[24,31,39] Alternatively, because cholesterol depletion increases cortical actin,[21] this may also lead to larger traction stresses, as observed in 3D collagen gels[6] and therefore, the cell may appear stiffer.[31] Indeed, a strong association between increased cell stiffness and tensile stress has been reported for human airway smooth muscle cells, even though the study did not focus on cholesterol modification.[16] This suggests that identification of individual cell traction forces from cholesterol-modified cells is necessary to properly elucidate the association among cholesterol depletion, membrane stiffness and traction stresses.

Lipid organization and cholesterol content is not only critical at the single-cell level, but appears just as important in monolayer formation and regulation. For example, in cow pulmonary endothelial cells, the plasma membrane of the cells undergo functional and structural changes as the cells become a confluent monolayer. This includes an increase in the membrane cholesterol, adherens junctions formation, and tyrosine dephosphorylation of adherens junctions proteins (AJPs).[11] This dephosphorylation is necessary for the formation of confluent endothelial monolayers, since increased tyrosine phosphorylation of AJPs results in the disruption of adherens junctions.[43,48] In cholesterol-enriched and untreated confluent cells, immunofluorescence staining of AJP pp120 was concentrated along adherens junctions. However, cholesterol depletion on confluent cells resulted in diffuse cytoplasmic staining and large gaps between adjacent cells. The observed results indicate that cholesterol depletion of confluent cells results in plasma membrane retraction from cell–cell interaction sites and disruption of adherens junctions by inducing tyrosine phosphorylation of AJPs. However, the mechanisms of cholesterol regulation on formation of confluent cells and stability of adherens junctions remain unknown.[11]

Based on recent studies, which have shown that cholesterol depletion in human aortic endothelial cells increases cellular stiffness and force generation[6] and decreases L27 cell adhesion to fibronectin-coated substrates, [32] we hypothesize that a similar effect will be seen in BAEC traction stresses, i.e. cholesterol depletion from cells increases the force that cells exert on the substrate. In turn, these larger forces translate into cell traction, which affects monolayer stability and cell spreading. We investigated the role of cholesterol in the force

exerted by BAECs on polyacrylamide gels using traction force microscopy. Independently, we also studied the effect of cholesterol on cell adhesion and spreading dynamics, using total internal reflection fluorescence and interference reflection microscopy (IRM) to visualize the adhesive contact between the cell membrane and the substrate. Our results show that the total average traction force generated by cells increases in cholesterol-depleted cells and remains the same in cholesterol-enriched cells. The average size of focal adhesions for single cells depleted of cholesterol also increases. Interestingly, we report a decrease in the spreading area of both single cells and monolayers for cholesterol-depleted cells. During spreading, depleted cells spread statistically less than controls, while enriched cells were not statistically different. Cell spreading is prevented initially due to an increase in cortical actin, and is likely further affected due to increased traction forces and adhesions at later times. Our results emphasize the importance of cholesterol in controlling and regulating the mechanical properties of the actin–plasma membrane complex, and the cellular mechanisms required for spreading.

METHODS

Cell Culture

Bovine aortic endothelial cells (BAECs) were purchased from Cambrex (East Rutherford, NJ) and cultured in Dulbecco's Modified Eagle's Medium supplemented with 10% fetal bovine serum, 1% 200 mM L-glutamine, and 0.5% penicillin–streptomycin (Invitrogen, Carlsbad, CA). The cells were maintained at 37 °C, 70% humidity, and 5% CO_2 and passaged every 5–7 days. All experiments were performed with cells between passages 3–9. Cells were plated on polyacrylamide (PA) gels for traction force microscopy measurements, or glass coated with 0.1 mg/mL fibronectin (Sigma–Aldrich, St. Louis, MO) for interference reflection microscopy (IRM) and total internal reflection fluorescence (TIRF) microscopy measurements.

Coverslip Activation and Polyacrylamide Gel Preparation

Cover slips were chemically activated to allow covalent attachment of PA sheets as described previously. [49] Briefly, coverslips (No. 1.5, 45 × 50 mm, Fisher Scientific, Pittsburgh, PA) were coated with a thin layer of 0.1 N NaOH, and coated with an additional layer of 3-aminopropylmethoxysilane (Sigma–Aldrich). Cover slips were rinsed with distilled water, then incubated in 0.5% glutaraldehyde (Sigma–Aldrich) for 30 min on a rocker, and rinsed again.

Acrylamide gels were prepared as described elsewhere [34] with a few modifications. Briefly, thin sheets of PA gel were prepared and adhered to the activated cover slips. A solution containing 5% acrylamide (40% w/v solution, Bio-Rad, Hercules, CA), 0.1% *N*,*N*′-methylene-bis-acrylamide (2% w/v solution, Bio-Rad), distilled water, and 1 M HEPES were made. Fluorescent latex spheres (1 μm Flurospheres, Molecular Probes, Eugene, OR) were added to the acrylamide solution in volume ratio of 1:100. After the solution was degassed, polymerization was initiated by addition of 1:200 volume of ammonium persulfate (10% w/v solution, Bio-Rad) and 1:20,000 volume of *N*′-Tetramethylethylene diamine. Afterward, the acrylamide solution was placed onto a circular cover slip (No. 1.5, 22-mm diameter, Fisher Scientific, Pittsburgh, PA) and the activated cover slips were placed on top. The resulting assembly was turned upside-down and polymerized for 45 min. The circular cover slip was removed and the gel was rinsed with 50 mM HEPES. Then, 250 μL of 0.1 mg/mL fibronectin solution (Sigma–Aldrich) was placed on the activated gel. After 2 h, the gel was rinsed with PBS and further incubated in 300 μL pf ethanolamine diluted 1:100 in PBS + 50 mM HEPES at room temperature for 30 min, and finally sterilized with

UV radiation. The thickness of the polyacrylamide gel was estimated to be 80 μm with a Young's modulus of 2,500 Pa as characterized previously.[34]

Cholesterol Treatment

BAECs were rinsed with serum-free DMEM and the cholesterol content was modified by incubating for 1 h in methyl-β-cyclodextrin (MβCD) saturated with cholesterol (enrichment), MβCD not complexed with cholesterol (depletion), and MβCD/MβCD–cholesterol mixture at a molar ratio that the level of cellular cholesterol was identical to the untreated cells (control). [10,25] The cells were rinsed again with serum-free DMEM after cholesterol treatment.

For spreading experiments, cells were plated in the presence of cholesterol enrichment or depletion; 2 mL of (MβCD) saturated with cholesterol, and without cholesterol, respectively was added to a fibronectin-coated glass bottom dish (No. 1.5, MatTek Co., Ashland, MA). Control cells were exposed to MβCD/MβCD–cholesterol mixture at a molar ratio that the level of cellular cholesterol was identical to the untreated cells during spreading experiments. For all experiments, cholesterol depletion, enrichment and control were performed in the same manner (as described above) and observed after 1 h to ensure identical conditions.

Fluorescence Labeling of BAEC Monolayers

Cells were plated onto fibronectin-coated glass-bottom dishes and reached confluence within 2 days. After cholesterol treatment, the monolayers were stained for 3 min using a lipophilic probe (lipid analog) 5 μM of 1,1′-dihexadecyl-3,3,3′,3′-tetramethylindocarbocyanine perchlorate ($DiIC_{16}$) in DMEM. The monolayers were rinsed with PBS and fixed with 2% paraformaldehyde for 20 min at room temperature before a final rinse with PBS.

Traction Force Microscopy

Traction force microscopy is a common method to measure the forces exerted by cells on compliant substrates. [2,4,13,16,47] Here, we used the method developed by Dembo and Wang, where the traction forces generated by migrating cells on the underlying substrate were quantified based on the displacements of the beads embedded in the substrate.[13] Briefly, cells are plated on PA gels embedded with fluorescent markers and the cells are allowed to adhere and spread on the substrate for 24 h. Fluorescent and phase contrast images of the spread cells and embedded beads are captured. Finally, the cells are removed using trypsin–EDTA and the final fluorescence images of the relaxed markers are captured. Based on the properties of the PA gel and the bead displacements, the traction forces can be calculated using the technique described by Dembo and Wang.[13] As previously described,[44] the overall force of the cell, $|F|$; is an integral of the traction field magnitude over the area, $|F|=\int\int \sqrt{T_x^2(x,y)+T_x^2(x,y)}dxdy$ where $\mathbf{T}(x,y) = [T_x(x,y), T_y(x,y)]$ is the continuous field of traction vectors defined at any spatial position (x,y) within the cell.

Interference Reflection Microscopy

IRM is based on the interference between the light reflected at the surface of the substrate and that reflected by the basal membrane of the cell.[12] The interference pattern of dark and bright fringes provides information on the cell adhesion to the substrate or the height distribution of the cell membrane lower surface. The dark areas correspond to the area where the cell membrane is closest to the substrate (tight adhesion/attachment). An inverted microscope (Olympus American Inc, Center Valley, PA) fitted with both 60× and 100× oil

immersion objective lenses and a 100 W mercury lamp (Olympus) was used for cell observations. Images were recorded with a CCD camera (Retiga SRV camera, QImaging, Surrey, BC Canada), and time lapse spreading experiments were performed in a closed microscope chamber (Precision Plastics, Inc, Beltsville, MD) to ensure characteristic culture conditions including 37 °C, 5% CO_2 and 50% humidity.

Total Internal Reflection Fluorescence Microscopy

TIRF microscopy has become a recently attractive method in assessing cell–substrate interactions[14,20] due to its ability to excite only fluorophores near the surface. [1] Single BAECs were fixed as described above for monolayers and stained for vinculin using first a 1:200 dilution of Anti-vinculin primary antibody (Sigma), followed by a 1:200 dilution of Alexa-fluor 488 Anti-mouse secondary antibody (Invitrogen). TIRF images were captured on an inverted microscope (Olymspus) fiber-optically coupled with two ion lasers (Melles Griot, Rochester, NY) for 488 and 561 nm excitation, and a CCD camera (Rolera-MGi, QImaging).

Data Analysis

For spreading area measurements of single cells, ImageJ (National Institutes of Health, Bethesda, MD) software was used to trace the cell borders and to quantify the total area. To quantify the area covered by the cells of control and treated monolayers, the light intensity threshold analysis of ImageJ software was used. In brief, snapshots were taken of 13–15 locations on separate monolayers after treatment and fixing procedure as mentioned above. These fluorescent snapshots were converted into binary images, which distinguished cell adhesion areas (fluorescent due to DiIC staining) vs. gaps in the monolayer (black). The amount of surface coverage from these binary images (not including gaps in the monolayer) is referred to as the average monolayer area.

ImageJ was also used for the quantification of the average vinculin adhesion area. All images were converted to binary images to isolate individual vinculin adhesions, and the particle analyzer in ImageJ was used to detect all adhesions greater then 0.5 μm_2 to prevent the quantification of background noise. The average vinculin adhesion area was recorded for each individual cell.

RESULTS AND DISCUSSION

Cholesterol-Depletion Increases the Average Traction Force

Traction force microscopy was used to measure the total average force exerted by endothelial cells on polyacrylamide (PA) gel substrates. Figure 1a shows an endothelial cell on a PA gel with 1 μm fluorescent embedded beads and the corresponding traction map in pseudocolor (Fig. 1b), indicating regions of low and high traction stresses in Pascals (dark blue to light pink). The traction forces were determined based on displacements of the embedded beads due to deformations on the gel surface, and the colored map indicates that the traction stresses are larger at the edges of the cell. The localization of larger traction stresses at the edge of the cell is consistent with previous work,[34] where it was shown that increased traction stresses exists underneath actin-rich pseudopodia compared to areas of adhesion underneath the nucleus. Note that cells that had no contact with adjacent cells were chosen to ensure no cell–cell interaction effect on cell spreading area and traction force. Traction forces were quantified in this manner for both cholesterol-depleted (cells treated with methyl-β-cyclodextrin (MβCD)) and cholesterol-enriched cells (MβCD saturated with cholesterol) as well as control cells (MβCD/MβCD–cholesterol mixture at a molar ratio that the level of cellular cholesterol was identical to the untreated cells).

The average total force exerted by cells onto the PA gel was statistically greater in cholesterol-depleted cells, with an almost two-fold increase compared to control and cholesterol-enriched cells (Fig. 1c). No statistical differences occur between control and cholesterol-enriched cells. This is in agreement with work that shows no significant effect of cholesterol enrichment on the membrane stiffness[5]; therefore, we would not expect to see increases in traction forces. Although force and cell spreading area vary among individual cells, it has been shown that these are dependent variables,[34] meaning that cells with increased areas exert increased traction forces. In this study, we specifically chose cells of similar spreading areas when performing traction force microscopy, which ensures that the increase in traction forces with cholesterol-depleted cells is not due to an increase in cell spreading area. To ensure that selected cells were characteristic of the entire population, cells were blindly selected within one standard deviation from the mean of the entire population. Figure 1d illustrates that for the cells which were selected, there are no statistical differences in the average area among control, cholesterol-depleted, or cholesterol-enriched cells. Note, that this does not suggest that cholesterol modification does not affect the cell spreading area, but rather that cells observed for force traction experiments were selected with similar areas to ensure that increased traction forces is not a result of increased spreading area. In addition to increased membrane stiffness for cholesterol depleted cells, it is possible that increased cell–substrate adhesion may contribute to the observed increases in traction forces, as many others have shown close relationships between focal adhesions and force.[2,3,40] To further evaluate this possibility, we used total internal reflection fluorescence (TIRF) microscopy to quantify cell–substrate adhesion.

Cholesterol-Depletion Increases Focal Adhesion Size

Earlier studies have shown an association between increased forces and increased focal adhesions.[2,38,47] Focal adhesions are involved in anchoring cells to the extracellular matrix substrates via actin–myosin and integrin receptors. These mechanosensitive cellular features can modify their shape, size and distribution in response to applied stress.[2,35] Due to the observed increase in traction forces for cholesterol-depleted cells, one would expect to see a potential increase in focal adhesion formation. To further understand the effect of cholesterol treatment on focal adhesions, vinculin (a focal adhesion protein) staining was observed using TIRF.

Vinculin staining is displayed in Fig. 2a for a characteristic cell using TIRF microscopy. ImageJ software was used to create binary images and to identify individual vinculin adhesion sites (Fig. 2b). The contact area of each vinculin site was quantified for each cell (as described in the Methods section) and the average size for each treatment is reported in Fig. 2c. The average contact area of individual vinculin adhesion sites is significantly increased in cholesterol-depleted cells, compared to cholesterol-enriched and control cells. No differences appear between control and cholesterol-enriched cells. This is consistent with earlier studies[2] and confirms the suspected relationship between increased focal adhesions and increased traction forces.

In addition to focal adhesions, stress fibers are also associated with traction forces.[45] Although it was previously reported that BAECs do not display differences in actin intensity when depleted of cholesterol, [5] we repeated these experiments by fixing cells and staining with phalloidin-TRITC. We then used TIRF microscopy to quantify the amount of actin fluorescence for control, depleted and enriched cells. Consistent with this previous work,[5] we do not see any significant differences in the actin intensity between control and cholesterol modifications (data not shown). Collectively, this illustrates that although it appears that focal adhesions (as determined through vinculin staining) contribute to the observed increased traction forces, it does not appear to be the case for actin. Note that force traction experiments are performed on compliant substrates, and TIRF microscopy is

performed using glass substrates; therefore the formation of focal adhesions may be magnified on glass, since others have observed increased vinculin staining on increased stiffness.[18,22] However, we do not have reason to suspect that the relationship between treatments would change. To further elucidate these concepts, future approaches would require a more thorough understanding of how cholesterol modification may be altered on substrates of varying stiffness.

To determine whether cell–substrate spreading area changes during the process of cholesterol depletion, as previously shown by Ramprasad *et al.* for L27 cells,[32] snapshots were captured using IRM during cholesterol depletion at 10 min intervals. As expected, well spread cells depleted of cholesterol detached significantly from the substrate during the first 20 min of incubation, however after 20 min detachment ceased (data not shown). Cells remain statistically less adhered for the remainder of the observed hour, illustrating that cholesterol depletion decreases the spreading area of single cells. Figure 3 illustrates the significant decrease in spreading area for cholesterol-depleted cells plated on glass, while no differences are observed between control and cholesterol-enriched cells. Collectively, this data shows that increased traction forces are associated with an increase in focal adhesion and also cell–substrate detachment.

Cholesterol Treatment Affects Spreading Behavior

As previously mentioned, cholesterol depletion has been shown to increase cortical F-actin,[21] and plasma membrane stiffness.[5,6] Increased membrane stiffness and cortical actin concentration suggest that cholesterol depletion may cause decreased cell spreading. The increase in cortical actin might result in an increase of cellular tension. This increase in tension can inhibit the initial cell spreading stages,[33] and may result in less spread cells. The increase in traction forces and adhesion for cholesterol-depleted cells are additional variables which may contribute to the inhibition of spreading (by increasing forces which oppose lamellipodial spreading); however, these variables would be involved later in the spreading process.

The effect of cholesterol on cell spreading was identified by observing spreading behavior during the process of cholesterol depletion or enrichment. To do so, cells were detached from the substrate as described for continuous passaging, and plated immediately onto freshly fibronectin-coated glass bottom dishes filled with MβCD saturated with cholesterol (enrichment) without cholesterol (depletion), or vehicle (control). Cells were left undisturbed for 1 h, and individual cells were then first identified using bright field microscopy to ensure single cells. Snapshots were taken using IRM to determine total spreading area.[41] The average spreading area for each condition is illustrated in Fig. 4. As expected, statistical differences in total spreading area are observed between cholesterol-depleted and control cells, as well as cholesterol-depleted and cholesterol-enriched cells ($p<0.01$, Student's t test). No differences are observed between cholesterol-enriched and control cells. Although previous experiments illustrate no difference in cell areas between control and cholesterol-depleted cells after 24 h,[23] we do report differences during the first hour of spreading. Since cells continuously regulate cholesterol levels over time in order to maintain homeostasis, we observe the early stages of spreading to ensure that cells do not have time to properly modify cholesterol content.

Cholesterol depletion decreases spreading area more than 30% compared to controlled cells (Fig. 4). This dramatic effect is consistent with others who show decreased motility and adhesion to fibronectin-coated substrates.[32] This group shows that cholesterol depletion in L27 cells plated onto fibronectin-coated surfaces resulted in the disappearance of lamellipodia and stress fibers, and an increase in cortical actin concentration. This indicates higher cortical tension (known to inhibit spreading[33]) and decreased motility, in agreement

with the decrease we observe during the first hour of spreading for cholesterol-depleted cells. Also of importance, Ramprasad *et al.*[32] show that actin stress fibers were reformed when membrane cholesterol content was restored, suggesting that the changes observed in motility and adhesion are related to the reorganization of the actin cytoskeleton. Therefore, cholesterol does not appear to have a direct effect on actin polymerization, but rather on the organization of F-actin cytoskeleton and membrane stiffness at the leading edge of the lamellipodia,[32] critical components of cell spreading.

The increase in cell–substrate adhesion that we report above (Fig. 2) correlates with the increased cytoskeleton–membrane adhesion occurring after cholesterol depletion, which is expected to significantly affect cell functions, including endocytosis.[46] It is suspected that this increase in adhesion makes it difficult for cells to form endocytic vesicles and therefore, the rate of endocytosis is decreased. This reduction in endocytosis would agree with our decreased spreading rates, since various endocytic pathways have been associated with spreading and ruffling.[7] In addition to endocytosis, exocytosis has also been shown as a critical component of the cell spreading process, by aiding to increase the plasma membrane area.[17] Others have suggested that cholesterol and sphingolipid-rich microdomains of alveolar epithelial type II cells serve as functional platforms during exocytosis.[9] When these cells were depleted of cholesterol, exocytosis was inhibited.[9] Together these results suggest that cholesterol depletion can cause a decrease in exocytosis, which in turn reduces the spreading area, consistent with our observation (Fig. 4). In addition, others have previously shown that depletion of cholesterol from the plasma membrane of fully spread cells causes a reduction in cell adhesion and motility.[32] Our measurements further support these observations by showing decreased spreading for cells depleted of cholesterol. This data emphasizes the important relationship between membrane composition, adhesion and cell spreading.

Monolayer Area Decreases with Both Cholesterol Depletion and Enrichment

Endothelial cells approaching confluence undergo intense structural and functional alterations, including a threefold increase in cholesterol levels and the formation of adherens junctions.[11] This significant increase in cholesterol levels suggests a critical role of cellular cholesterol in regulatory pathways involved in cell–cell interactions and plasma membrane regulation. Previous studies have shown that cholesterol depletion on confluent cells disrupts intercellular junctions, and causes cell detachment,[11,19] however, specific cell–substrate interactions and retraction behavior is not completely clear. In our study, we aimed to observe the effect of cholesterol treatment on BAEC confluent monolayers plated on fibronectin-coated glass, by observing the changes in cell–substrate and cell–cell adhesion over the course of 1 h. The cholesterol treatment includes control, and 30 and 60 min cholesterol-depleted and enriched confluent cells. The confluent monolayers were stained with lipid analog $DiIC_{16}$ and fixed with 2% paraformaldehyde. Images of the monolayers were captured and ImageJ software was used to quantify the total monolayer area after treatment.

Figure 5a shows the average monolayer area and indicates that cholesterol depletion significantly reduces the average monolayer area compared to control monolayer. This effect is even more pronounced for a longer time period of cholesterol depletion. Statistical differences are reported between cholesterol depletion at 30 min compared to 60 min (Student's *t* test, $p<0.05$). Within 30 min of incubation, cholesterol enrichment also significantly decreases the average monolayer area. Representative monolayer images after 60 min of treatment are shown in Fig. 5b, with the identified boxed region magnified in Fig. 5c. For the control cells, the monolayer remains intact, as illustrated by the continuous cell coverage and very little substrate (black) observed. For cholesterol depleted cells, some cells have rounded up and are almost entirely detached from the substrate (white arrow). This

observed detachment of the endothelial sheets is also consistent with the behavior observed for single cells, which slightly retract from the surface during cholesterol depletion as mentioned above and displayed in Fig. 3. Cell–substrate detachment is also noticed in cholesterol-enriched monolayers, although to a lesser degree. Cell–cell detachment is observed in both cholesterol-enriched and cholesterol-depleted monolayers and can be easily distinguished based on tethering observed between cell groups (Fig. 5c). This illustrates that both cholesterol enrichment and depletion affect the average monolayer area, with 60 min of cholesterol depletion having the most dramatic influence.

Since cholesterol-depleted cells show a decrease in spreading area for both single cells (Fig. 3) and monolayers (Fig. 5), it was of interest to determine whether the increase in focal adhesions observed for single cells (Fig. 2) was retained in cholesterol-depleted monolayers. Control, as well as cholesterol-depleted and cholesterol-enriched monolayers were fixed and stained for vinculin as described for single cells. However, no difference in the average size of focal adhesions was identified among the treated monolayers compared to control (data not shown). This is contrary to the effect observed in single cells; however, it is not entirely surprising due to differences in integrin clustering, actin organization, spreading area and/or force traction, which are all variables that can affect adhesion and focal adhesion morphology.[2,15,34,50] In addition, differences in the integrity of the monolayer (as shown in Fig. 5) due to cholesterol modification may affect focal adhesion morphology for monolayers.

In sum, these observations confirm that cholesterol is a critical component in the proper formation of cell–cell and cell–substrate contacts necessary to maintain BAEC monolayers. Endothelial sheets serve in a variety of ways to maintain essential vascular tissue physiology by helping to regulate blood clotting and blood vessel diameter, and by serving as a barrier which selectively allows for the transport of molecules between blood and tissue surfaces.[11,29] The endothelium also functions as a critical component of the immune response system by regulating leukocyte docking and transmigration.[11] Our results illustrate that cholesterol-depletion (as well as enrichment) compromises the integrity of the endothelial barrier by inducing cell–cell and cell–substrate detachment.

CONCLUSIONS

This paper demonstrates that cholesterol depletion from BAECs increases the force that cells exert on the substrate. In turn, these increased cell tractions affect individual cell spreading dynamics, adhesion and monolayer stability. Our results emphasize the importance of cholesterol in controlling and regulating the mechanical properties of the actin–plasma membrane complex, and the cellular mechanisms required for spreading. In addition, these results suggest that cellular cholesterol has global effects on cell properties through changes in actin cytoskeleton, beyond the local membrane environment. Interaction of the cell membrane with the underlying cytoskeleton (membrane–cytoskeleton adhesion) has a major impact on vital cell functions, such as endocytosis, exocytosis, membrane extension and retraction, cell morphology, and migration.[42] Ultimately, the results we present here emphasize the importance of cholesterol in regulating cell adhesion and spreading as well as monolayer structure and maintenance. Additional studies correlating the relationship between cellular changes following cholesterol modification and the signaling pathways which may relate these changes to disease will be of significant interest in relation to treatments for atherosclerosis and lipid organization disorders.

Acknowledgments

The authors thank Elena Tous for assistance with monolayer staining and preparations. This work was supported by NSF Grant CMMI-0643783 to HAE, National Institutes of Health Grants HL083298 and HL073965 to IL, and a Department of Defense CREST Graduate Fellowship to LLN.

REFERENCES

1. Axelrod D. Total internal reflection fluorescence microscopy in cell biology. Methods Enzymol. 2003; 361:1–33. [PubMed: 12624904]
2. Balaban NQ, Schwarz US, Riveline D, Goichberg P, Tzur G, et al. Force and focal adhesion assembly: a close relationship studied using elastic micropatterned substrates. Nat. Cell Biol. 2001; 3:466–472. [PubMed: 11331874]
3. Bershadsky AD, Balaban NQ, Geiger B. Adhesion-dependent cell mechanosensitivity. Annu. Rev. Cell Dev. Biol. 2003; 19:677–695. [PubMed: 14570586]
4. Butler JP, Tolic-Norrelykke IM, Fabry B, Fredberg JJ. Traction fields, moments, and strain energy that cells exert on their surroundings. Am. J. Physiol. Cell Physiol. 2002; 282:C595–C605. [PubMed: 11832345]
5. Byfield FJ, Aranda-Espinoza H, Romanenko VG, Rothblat GH, Levitan I. Cholesterol depletion increases membrane stiffness of aortic endothelial cells. Biophys. J. 2004; 87:3336–3343. [PubMed: 15347591]
6. Byfield FJ, Tikku S, Rothblat GH, Gooch KJ, Levitan I. OxLDL increases endothelial stiffness, force generation, and network formation. J. Lipid Res. 2006; 47:715–723. [PubMed: 16418538]
7. Cavalli V, Corti M, Gruenberg J. Endocytosis and signaling cascades: a close encounter. FEBS Lett. 2001; 498:190–196. [PubMed: 11412855]
8. Chen M, Mason RP, Tulenko TN. Atherosclerosis alters the composition, structure and function of arterial smooth-muscle cell plasma-membranes. Biochim. Biophys. Acta. 1995; 1272:101–112. [PubMed: 7548233]
9. Chintagari NR, Jin N, Wang P, Narasaraju TA, Chen J, Liu L. Effect of cholesterol depletion on exocytosis of alveolar type II cells. Am. J. Respir. Cell Mol. Biol. 2006; 34:677–687. [PubMed: 16439800]
10. Christian AE, Haynes MP, Phillips MC, Rothblat GH. Use of cyclodextrins for manipulating cellular cholesterol content. J. Lipid Res. 1997; 38:2264–2272. [PubMed: 9392424]
11. Corvera S, DiBonaventura C, Shpetner HS. Cell confluence-dependent remodeling of endothelial membranes mediated by cholesterol. J. Biol. Chem. 2000; 275:31414–31421. [PubMed: 10903311]
12. Curtis ASG. Mechanism of adhesion of cells to glass—study by interference reflection microscopy. J. Cell Biol. 1964; 20:199. [PubMed: 14126869]
13. Dembo M, Wang YL. Stresses at the cell-to-substrate interface during locomotion of fibroblasts. Biophys. J. 1999; 76:2307–2316. [PubMed: 10096925]
14. Dubin-Thaler BJ, Giannone G, Dobereiner HG, Sheetz MP. Nanometer analysis of cell spreading on matrix-coated surfaces reveals two distinct cell states and STEPs. Biophys. J. 2004; 86:1794–1806. [PubMed: 14990505]
15. Engler A, Bacakova L, Newman C, Hategan A, Griffin M, Discher D. Substrate compliance versus ligand density in cell on gel responses. Biophys. J. 2004; 86:617–628. [PubMed: 14695306]
16. Galbraith CG, Sheetz MP. A micromachined device provides a new bend on fibroblast traction forces. Proc. Natl Acad. Sci. USA. 1997; 94:9114–9118. [PubMed: 9256444]
17. Gauthier NC, Rossier OM, Mathur A, Hone JC, Sheetz MP. Plasma membrane area increases with spread area by exocytosis of a GPI-anchored protein compartment. Mol. Biol. Cell. 2009; 20:3261–3272. [PubMed: 19458190]
18. Guo WH, Frey MT, Burnham NA, Wang YL. Substrate rigidity regulates the formation and maintenance of tissues. Biophys. J. 2006; 90:2213–2220. [PubMed: 16387786]
19. Ilangumaran S, Hoessli DC. Effects of cholesterol depletion by cyclodextrin on the sphingolipid microdomains of the plasma membrane. Biochem. J. 1998; 335:433–440. [PubMed: 9761744]

20. Joos U, Biskup T, Ernst O, Westphal I, Gherasim C, et al. Investigation of cell adhesion to structured surfaces using total internal reflection fluorescence and confocal laser scanning microscopy. Eur. J. Cell Biol. 2006; 85:225–228. [PubMed: 16546565]
21. Klausen TK, Hougaard C, Hoffmann EK, Pedersen SF. Cholesterol modulates the volume-regulated anion current in Ehrlich-Lettre ascites cells via effects on Rho and F-actin. Am. J. Physiol. Cell Physiol. 2006; 291:C757–C771. [PubMed: 16687471]
22. Kong HJ, Polte TR, Alsberg E, Mooney DJ. FRET measurements of cell-traction forces and nano-scale clustering of adhesion ligands varied by substrate stiffness. Proc. Natl Acad. Sci. USA. 2005; 102:4300–4305. [PubMed: 15767572]
23. Kowalsky GB, Byfield FJ, Levitan I. oxLDL facilitates flow-induced realignment of aortic endothelial cells. Am. J. Physiol. Cell Physiol. 2008; 295:C332–C340. [PubMed: 18562483]
24. Kwik J, Boyle S, Fooksman D, Margolis L, Sheetz MP, Edidin M. Membrane cholesterol, lateral mobility, and the phosphatidylinositol 4,5-bisphosphate-dependent organization of cell actin. Proc. Natl Acad. Sci. USA. 2003; 100:13964–13969. [PubMed: 14612561]
25. Levitan I, Christian AE, Tulenko TN, Rothblat GH. Membrane cholesterol content modulates activation of volume-regulated anion current in bovine endothelial cells. J. Gen. Physiol. 2000; 115:405–416. [PubMed: 10736308]
26. Levitan I, Gooch KJ. Lipid rafts in membrane–cytoskeleton interactions and control of cellular biomechanics: actions of oxLDL. Antioxid. Redox Signal. 2007; 9:1519–1534. [PubMed: 17576163]
27. Lundbaek JA, Birn P, Girshman J, Hansen AJ, Andersen OS. Membrane stiffness and channel function. Biochemistry. 1996; 35:3825–3830. [PubMed: 8620005]
28. Maxfield FR, Tabas I. Role of cholesterol and lipid organization in disease. Nature. 2005; 438:612–621. [PubMed: 16319881]
29. Michiels C. Endothelial cell functions. J. Cell. Physiol. 2003; 196:430–443. [PubMed: 12891700]
30. Needham D, Nunn RS. Elastic-deformation and failure of lipid bilayer-membranes containing cholesterol. Biophys. J. 1990; 58:997–1009. [PubMed: 2249000]
31. Pourati J, Maniotis A, Spiegel D, Schaffer JL, Butler JP, et al. Is cytoskeletal tension a major determinant of cell deformability in adherent endothelial cells? Am. J. Physiol. Cell Physiol. 1998; 43:C1283–C1289.
32. Ramprasad OG, Srinivas G, Rao KS, Joshi P, Thiery JP, et al. Changes in cholesterol levels in the plasma membrane modulate cell signaling and regulate cell adhesion and migration on fibronectin. Cell Motil. Cytoskeleton. 2007; 64:199–216. [PubMed: 17238130]
33. Raucher D, Sheetz MP. Cell spreading and lamellipodial extension rate is regulated by membrane tension. J. Cell Biol. 2000; 148:127–136. [PubMed: 10629223]
34. Reinhart-King CA, Dembo M, Hammer DA. Endothelial cell traction forces on RGD-derivatized polyacrylamide substrata. Langmuir. 2003; 19:1573–1579.
35. Riveline D, Zamir E, Balaban NQ, Schwarz US, Ishizaki T, et al. Focal contacts as mechanosensors: Externally applied local mechanical force induces growth of focal contacts by an mDia1-dependent and ROCK-independent mechanism. J. Cell Biol. 2001; 153:1175–1185. [PubMed: 11402062]
36. Romanenko VG, Rothblat GH, Levitan I. Modulation of endothelial inward-rectifier K+ current by optical isomers of cholesterol. Biophys. J. 2002; 83:3211–3222. [PubMed: 12496090]
37. Romanenko VG, Rothblat GH, Levitan I. Sensitivity of volume-regulated anion current to cholesterol structural analogues. J. Gen. Physiol. 2004; 123:77–87. [PubMed: 14699079]
38. Saez A, Buguin A, Silberzan P, Ladoux B. Is the mechanical activity of epithelial cells controlled by deformations or forces? Biophys. J. 2005; 89:L52–L54. [PubMed: 16214867]
39. Sato M, Theret DP, Wheeler LT, Ohshima N, Nerem RM. Application of the micropipette technique to the measurement of cultured porcine aortic endothelial-cell viscoelastic properties. J. Biomech. Eng. 1990; 112:263–268. [PubMed: 2214707]
40. Schwarz US, Balaban NQ, Riveline D, Bershadsky A, Geiger B, Safran SA. Calculation of forces at focal adhesions from elastic substrate data: the effect of localized force and the need for regularization. Biophys. J. 2002; 83:1380–1394. [PubMed: 12202364]

41. Sengupta K, Aranda-Espinoza H, Smith L, Janmey P, Hammer D. Spreading of neutrophils: from activation to migration. Biophys. J. 2006; 91:4638–4648. [PubMed: 17012330]
42. Sheetz MP, Sable JE, Dobereiner HG. Continuous membrane–cytoskeleton adhesion requires continuous accommodation to lipid and cytoskeleton dynamics. Annu. Rev. Biophys. Biomol. Struct. 2006; 35:417–434. [PubMed: 16689643]
43. Shibamoto S, Hayakawa M, Takeuchi K, Hori T, Oku N, et al. Tyrosine phosphorylation of beta-catenin and plakoglobin enhanced by hepatocyte growth-factor and epidermal growth-factor in human carcinoma-cells. Cell Adhes. Commun. 1994; 1:295–305. [PubMed: 8081883]
44. Smith LA, Aranda-Espinoza H, Haun JB, Dembo M, Hammer DA. Neutrophil traction stresses are concentrated in the uropod during migration. Biophys. J. 2007; 92:L58–L60. [PubMed: 17218464]
45. Solon J, Levental I, Sengupta K, Georges PC, Janmey PA. Fibroblast adaptation and stiffness matching to soft elastic substrates. Biophys. J. 2007; 93:4453–4461. [PubMed: 18045965]
46. Sun M, Northup N, Marga F, Huber T, Byfield FJ, et al. The effect of cellular cholesterol on membrane–cytoskeleton adhesion. J. Cell Sci. 2007; 120:2223–2231. [PubMed: 17550968]
47. Tan JL, Tien J, Pirone DM, Gray DS, Bhadriraju K, Chen CS. Cells lying on a bed of microneedles: an approach to isolate mechanical force. Proc. Natl Acad. Sci. USA. 2003; 100:1484–1489. [PubMed: 12552122]
48. Ukropec JA, Hollinger MK, Salva SM, Woolkalis MJ. SHP2 association with VE-cadherin complexes in human endothelial cells is regulated by thrombin. J. Biol. Chem. 2000; 275:5983–5986. [PubMed: 10681592]
49. Wang YL, Pelham RJ. Preparation of a flexible, porous polyacrylamide substrate for mechanical studies of culture cells. Methods Enzymol. 1998; 298:489–496. [PubMed: 9751904]
50. Yeung T, Georges PC, Flanagan LA, Marg B, Ortiz M, et al. Effects of substrate stiffness on cell morphology, cytoskeletal structure, and adhesion. Cell Motil. Cytoskeleton. 2005; 60:24–34. [PubMed: 15573414]

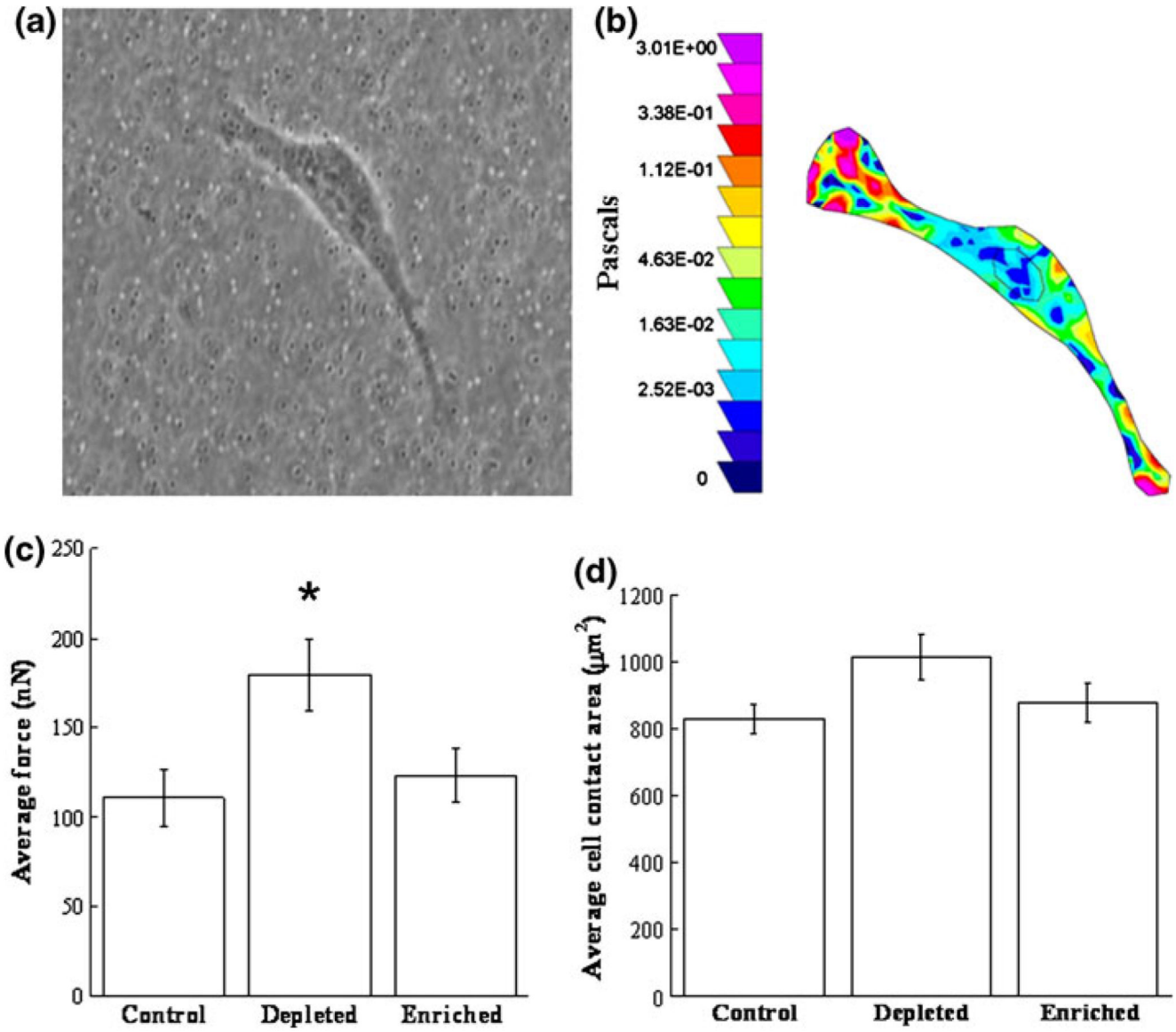

FIGURE 1.

Effect of cellular cholesterol on cell traction forces. (a) Bovine aortic endothelial cells (BAECs) were cultured onto polyacrylamide gels embedded with fluorescent beads for traction force microscopy. Cells spread for 24 h, and fluorescent images were taken before and after cell detachment. (b) Traction forces were quantified by measuring the bead displacements, and a corresponding color traction maps illustrates the largest forces appear at the cell edge. The pseudocolor bar represents traction stresses in Pascals. (c) Average force exerted by the cell for control (N = 18), cholesterol-depleted (N = 21), and cholesterol-enriched (N = 18) cells. The traction forces for cholesterol-depleted cells were statistically larger than the control and cholesterol-enriched cells (using Student's t test, with $p<0.05$). (d) No significant differences are observed in the average cell area for control (N = 18), cholesterol-depleted (N = 21), or cholesterol-enriched (N = 18) cells. Note this area represents the average spreading area only for cells selected for traction experiments, and does not represent the entire population of cholesterol treated cells. Error bars represent standard error.

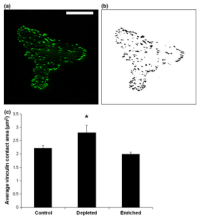

FIGURE 2.

Identification of the average vinculin contact area using total internal reflection fluorescence (TIRF) microscopy. (a) TIRF microscopy is used to identify vinculin adhesion sites close to the substrate. Scale bar is 25 μm. Binary images are created (b) and the area of each individual vinculin adhesion site is quantified. (c) The average vinculin adhesion area is significantly increased in cholesterol depleted cells compared to both control and cholesterol enriched cells (using Student's *t* test with $p<0.05$). No significant differences occur between control and cholesterol enriched cells. Error bars represent standard error (N = 28, 26, and 25 cells for control, depleted and enriched, respectively).

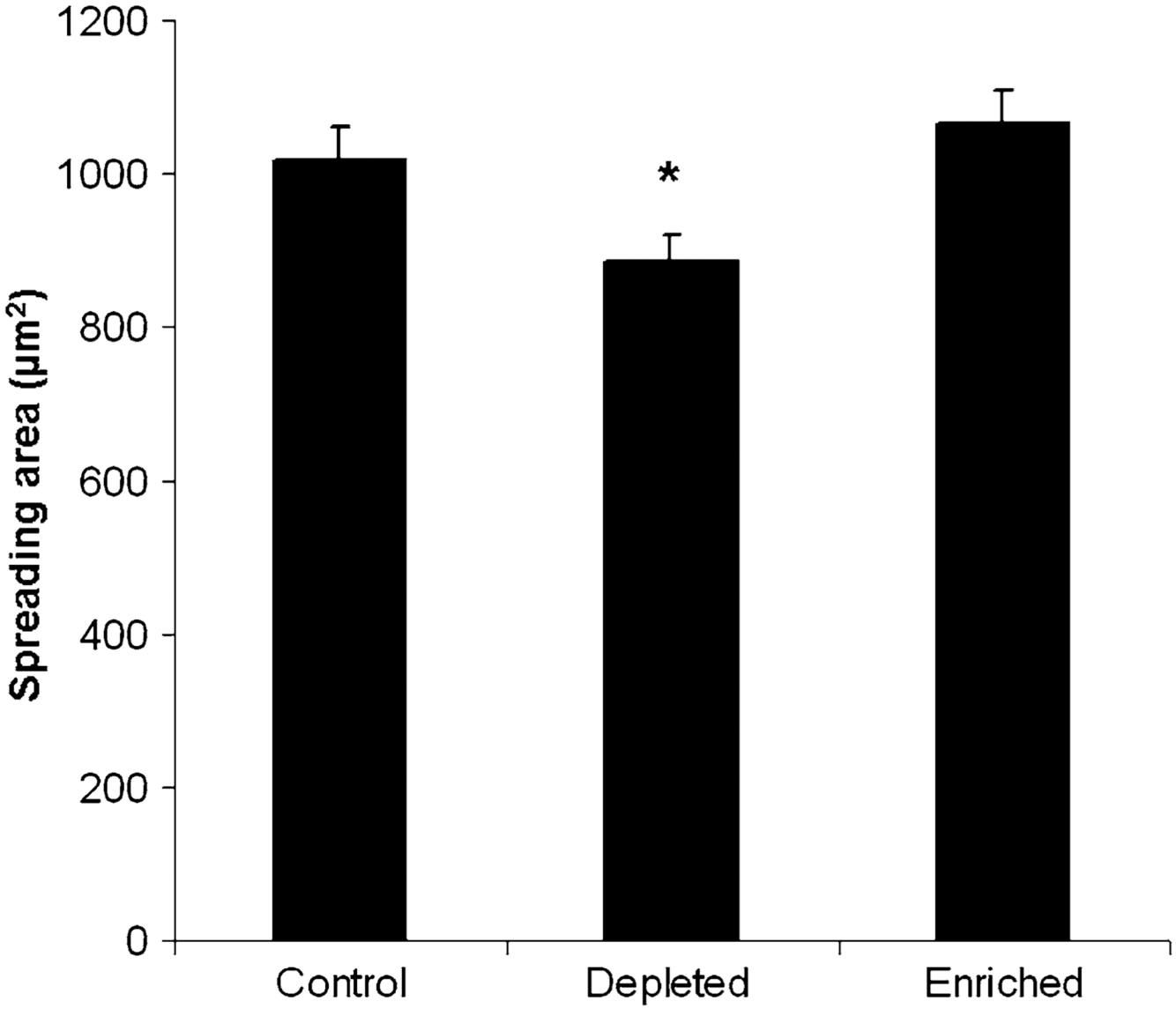

FIGURE 3.

Single cell spreading on fibronectin-coated glass substrates. Spread BAECs incubated for 1 h with control solution (1:1 MβCD:MβCD–cholesterol mixture), MβCD solution (depleted) or MβCD saturated with cholesterol solution (enriched), and are observed using IRM. Cells depleted of cholesterol are significantly less spread compared to control cells, while no differences are observed between control and cholesterol-enriched cells. Asterisk denotes significant difference using Student's *t* test with $p<0.05$. Error bars represent standard error (N = 36–44 cells per condition).

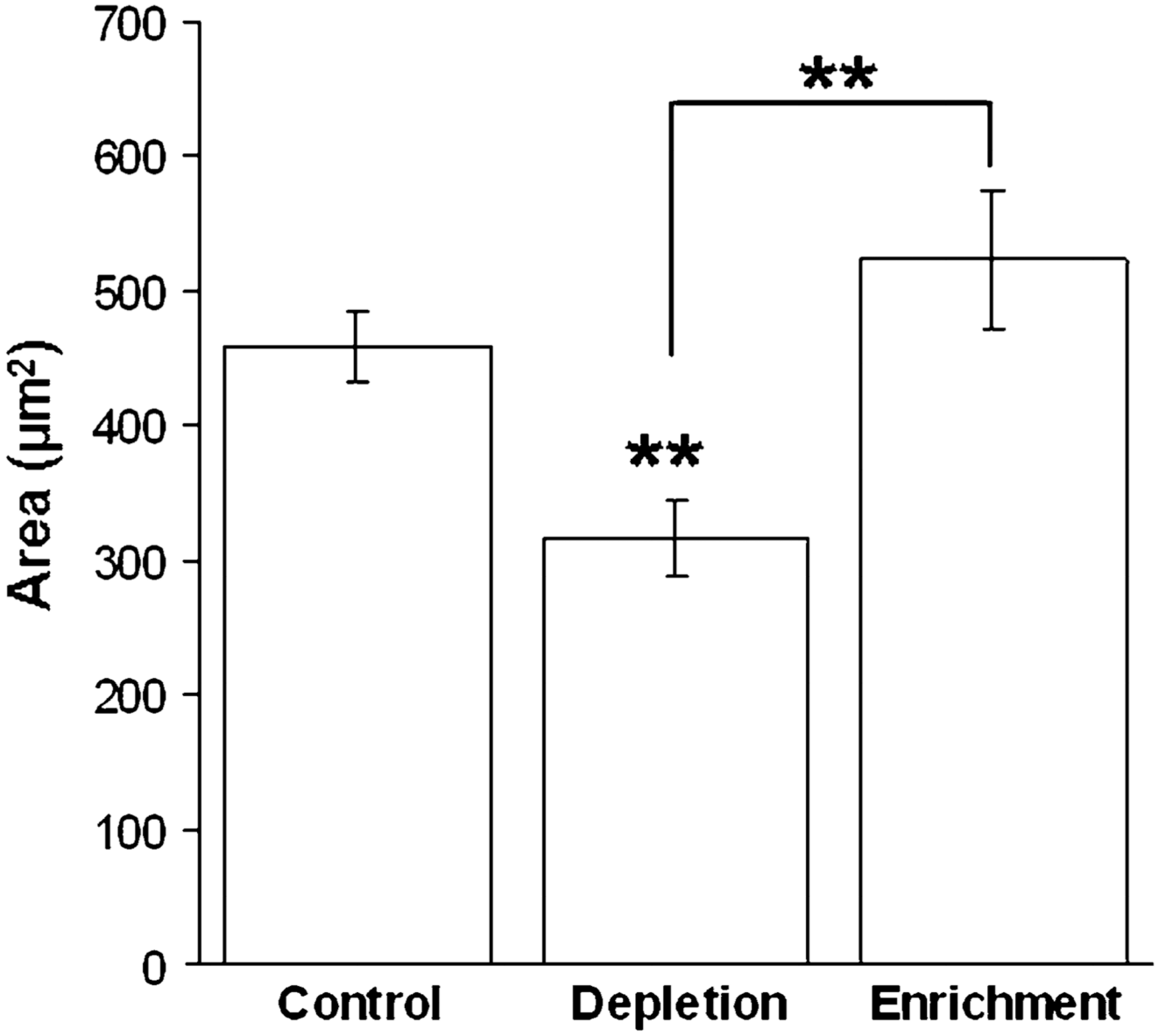

FIGURE 4.

Cells were plated onto fibronectin-coated glass bottom dishes containing control, cholesterol-depletion or cholesterol-enrichment solutions. Total spreading area was observed for untreated control cells ($N = 40$), cholesterol depleted ($N = 60$) and cholesterol enriched cells ($N = 53$) after 1 h of spreading using IRM. ImageJ was used to trace cell boundaries and quantify total spreading area. Error bars illustrate standard error with statistical significance reported using Student's t test ($p < 0.01$). Depleted cells are statistically less spread compared to control cells, while enriched cells are not statistically different.

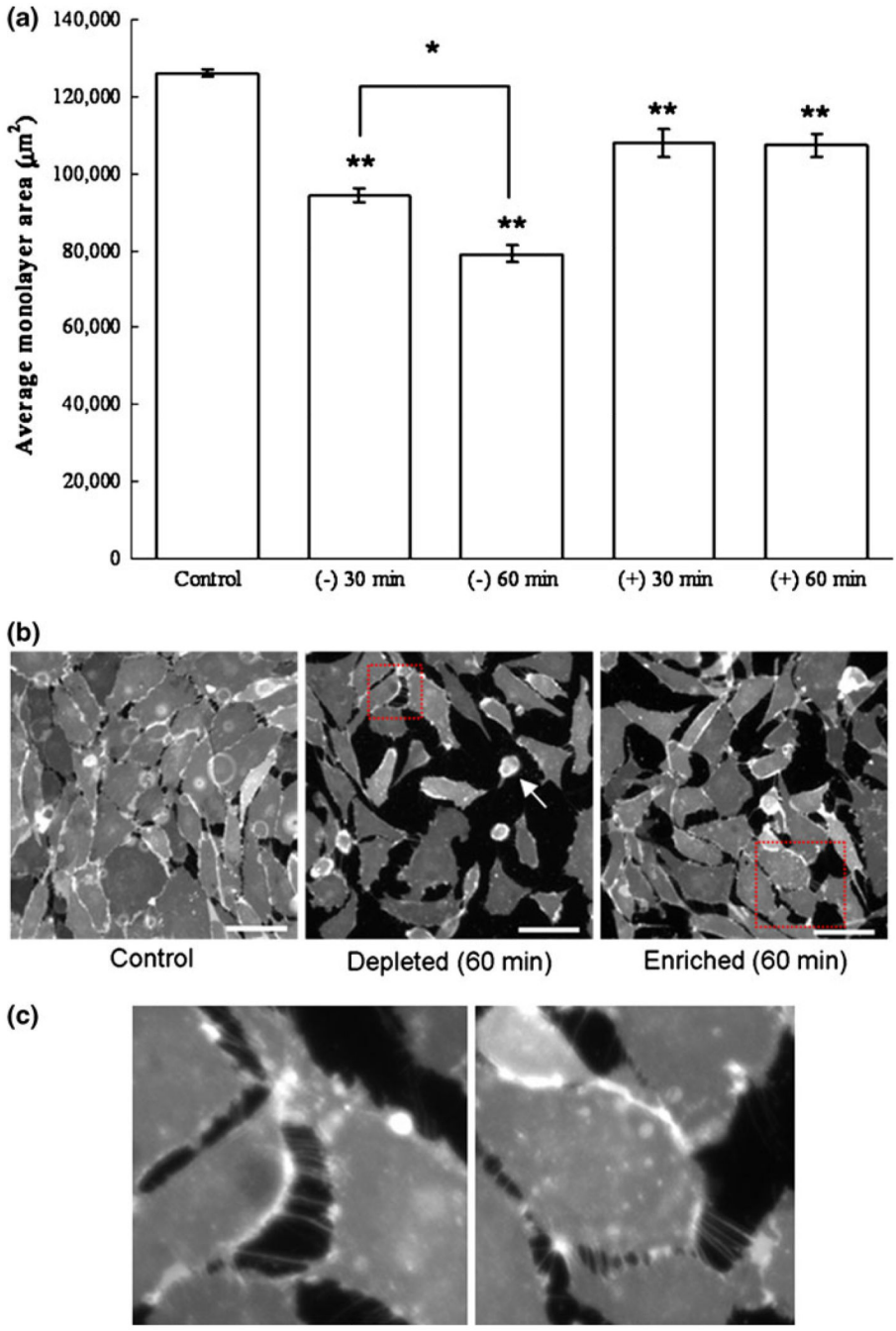

FIGURE 5.

Effect of cholesterol treatment on BAEC confluent monolayer plated on a fibronectin-coated glass for control, 30 min, and 60 min cholesterol-depleted (−) and cholesterol-enriched (+) cells (a). Monolayers were stained using the lipophilic probe DiIC[16], and fixed after their respective treatment as described in the Methods section. The average area of monolayer coverage was quantified for 13–15 separate monolayer areas using ImageJ thresholding software. Error bars represent standard error obtained from the experimental data points. Statistical significances of all cholesterol treatment from control experiment are reported at 95% confidence level using Student's *t* test (** $p < 0.01$, * $p < 0.05$). Representative images are shown for control, as well as cholesterol-ldepleted and cholesterol-enriched cells after 60

min of treatment. Scale bar is 50 μm. (b) After 60 min of cholesterol depletion, some cells have rounded up and are almost entirely detached from the substrate (white arrow). In addition to cell–substrate detachment, cell–cell detachment is also observed and can be distinguished based on tethering observed between cell groups (c). Tethering of cholesterol depleted cells (c, left) appears similarly as that for cholesterol enriched cells (c, right), suggesting that both treatments result in a disruption of cell–cell adhesion.